The Synthetic Cannabinoid R(+)WIN55,212-2 Augments Interferon-β Expression via Peroxisome Proliferator-activated Receptor-α*□S

Eric J. Downer[‡1,2], **Eileen Clifford**[‡], **Sylvie Amu**[§], **Padraic G. Fallon**[§], **and Paul N. Moynagh**[‡1,3]

From the ‡Institute of Immunology, National University of Ireland Maynooth, County Kildare, Ireland and the §Institute of Molecular Medicine, Trinity College Dublin, St. James's Hospital, Dublin 8, Ireland

Background: The synthetic cannabinoid R(+)WIN55,212-2 can regulate IFN-β expression.
Results: R(+)WIN55,212-2 regulates IFN-β expression in a PPARα-dependent manner.
Conclusion: PPARα mediates effects of R(+)WIN55,212-2 on IFN-β expression.
Significance: PPARα contributes to protective effects of R(+)WIN55,212-2 in models of multiple sclerosis.

We have demonstrated that R(+)WIN55,212-2, a synthetic cannabinoid that possesses cannabimimetic properties, acts as a novel regulator of Toll-like receptor 3 (TLR3) signaling to interferon (IFN) regulatory factor 3 (IRF3) activation and IFN-β expression, and this is critical for manifesting its protective effects in a murine multiple sclerosis model. Here we investigated the role of peroxisome proliferator-activated receptor-α (PPARα) in mediating the effects of R(+)WIN55,212-2 on this pathway. Data herein demonstrate that the TLR3 agonist poly(I:C) promotes IFN-β expression and R(+)WIN55,212-2 enhances TLR3-induced IFN-β expression in a stereoselective manner via PPARα. R(+)WIN55,212-2 promotes increased transactivation and expression of PPARα. Using the PPARα antagonist GW6471, we demonstrate that R(+)WIN55,212-2 acts via PPARα to activate JNK, activator protein-1, and positive regulatory domain IV to transcriptionally regulate the IFN-β promoter. Furthermore, GW6471 ameliorated the protective effects of R(+)WIN55,212-2 during the initial phase of experimental autoimmune encephalomyelitis. Overall, these findings define PPARα as an important mediator in manifesting the effects of R(+)WIN55,212-2 on the signaling cascade regulating IFN-β expression. The study adds to our molecular appreciation of potential therapeutic effects of R(+)WIN55,212-2 in multiple sclerosis.

Current multiple sclerosis (MS)[4] therapies are partially effective and are based on immunomodulation, restoration of blood brain barrier integrity, and repair of damage (1). The type I interferon (IFN), IFN-β, is a front line therapy currently available to treat patients with MS (2), displaying beneficial effects on disability progression (3) and relapse rate (4). IFN-β exerts a diverse array of therapeutic mechanisms, with demonstrated effects on antigen presentation, co-stimulatory molecule expression, T cell proliferation, and leukocyte migration (5). Given its clinical efficacy, an increased understanding of novel mechanisms that regulate endogenous expression of IFN-β may provide important clues to new therapy development.

Transcriptional regulation of IFN-β requires the assembly of a transcription enhancer complex on four positive regulatory domains (PRDI to -IV) (6). PRDI-III domains are recognized by IFN regulatory factors (IRFs) (3 and 7), PRDII by nuclear factor-κB (NF-κB) and PRDIV by activator protein-1 (AP-1) (ATF-2/c-Jun), and these transcription factors act in co-operation to form an enhanceosome that drives efficient production of IFN-β (7). Intriguingly, we have recently demonstrated that the aminoalkylindole, R(+)WIN55,212-2, regulates IFN-β expression by augmenting activation of IRF3 and this is critical for manifesting its protective effects in experimental autoimmune encephalomyelitis (EAE), an animal model of MS (8). R(+)WIN55,212-2 is a potent synthetic cannabinoid receptor agonist and while capable of binding to both CB$_1$ and CB$_2$ cannabinoid receptors, it exhibits greater selectivity for CB$_2$ (9). However, we have demonstrated cannabinoid receptor-independent mechanisms of action for R(+)WIN55,212-2, including those underlying its regulation of IFN-β expression (8). Such findings and others clearly indicate that R(+)-WIN55,212-2 can work independently of the classical cannabinoid receptor system. Indeed, other candidate receptors exist for mediating cannabinoid effects, including the orphan receptor GPR55 (10) and transient receptor potential vanilloid type 1 (TRPV1) (11). However more recent interest has focused on the role of nuclear receptor superfamily of peroxisome proliferator-activated receptors (PPARs) as potential mediators of some cannabinoid activity (12). Interestingly cannabinoid-mediated

[4] The abbreviations used are: MS, multiple sclerosis; AP-1, activator protein-1; EAE, experimental autoimmune encephalomyelitis; HEK, human embryonic kidney; NF-κB, nuclear factor-κB; PPAR, peroxisome proliferator-activated receptor; PPRE, PPAR response element; PRD, positive regulatory domain; TLR, Toll-like receptor; TRIF, Toll-interleukin-1 receptor domain-containing adaptor-inducing IFN-β; HPRT, hypoxanthine phosphoribosyl- transferase; RANTES, regulated on activation normal T cell expressed and secreted; PLP, proteolipid protein; TK, thymidine kinase.

anti-inflammatory propensity has been linked with PPAR activity (13–14) and this is consistent with the anti-inflammatory effects of PPAR ligands (15–16).

PPARs are ligand-activated nuclear receptors with effects on proliferation, metabolism and immunity (17). Three isoforms exist (PPARα, -γ, and −δ) which heterodimerize with the retinoid X receptor, activating transcription by binding a specific DNA element called the PPAR response element (PPRE) (17). The PPAR subtypes exhibit distinct tissue expression patterns (18), with expression characterized throughout the central nervous system (CNS) (19). PPAR agonists (thiazolidinediones) are used clinically in the treatment of diabetes and experimental evidence suggests potential clinical benefits for patients with neuroinflammatory disorders (20).

The anti-inflammatory properties of PPARs result, at least in part, from inhibition of transcription factors NF-κB and AP-1, and subsequent regulation of chemokines, cytokines and adhesion molecules (16, 21–22). Activation of transcription factors such as NF-κB, in addition to members of the IRF family, is tightly controlled by TLRs, single transmembrane receptors involved in the recognition of conserved microbial motifs (23). Despite the integral role of TLRs in pathogen recognition, dysregulation of TLR signaling cascades is associated with inflammation (24). We have previously demonstrated that *R(+)*WIN55,212-2 differentially regulates TLR signaling (TLR3 and TLR4), and in particular, this aminoalkylindole derivative acts as a novel regulator of TLR3 signaling to IRF3 and subsequent expression of IFN-β (8). Such effects of *R(+)*WIN55,212-2, in particular its capacity to induce endogenous IFN-β, offers an attractive additional option to the current use of exogenously administered IFN-β in MS. Indeed, a high percentage of patients fail to respond to current therapy, with treatment failure associated with production of neutralizing antibodies to IFN-β in some cases (25). However, cannabinoid receptor involvement was not associated with the effects of *R(+)*WIN55,212-2 on endogenous IFN-β expression. Given previous reports that cannabinoid compounds may manifest at least some effects via PPARα (13, 26) we were particularly interested to explore the role of PPARα in mediating the effects of *R(+)*WIN55,212-2 on IFN-β expression. We show that *R(+)*WIN55,212-2 promotes PPARα transactivation and expression, and potentiates TLR3-induced IFN-β via a PPARα mechanism. We further show that *R(+)*WIN55,212-2 specifically targets the AP-1-binding enhancer element of the IFN-β promoter, and this effect of *R(+)*WIN55,212-2 is reliant on the PPARα isoform. This study thus identifies a novel role for PPARα in regulating the signaling cascade leading to IFN-β expression.

EXPERIMENTAL PROCEDURES

Materials—The rabbit polyclonal antibodies recognizing phosphorylated and total JNK were from Cell Signaling Technology Inc. (Danvers, MA). The goat polyclonal PPARα antibody was from Santa Cruz Biotechnology Inc. (Santa Cruz, CA). The firefly luciferase NF-κB reporter construct was a gift from Prof. Luke O'Neill (Trinity College Dublin, Ireland). The pFR-luciferase Gal4 reporter construct was a gift from Prof. Andrew Bowie (Trinity College). Constructs encoding IRF3 Gal4

reporter and the IFN-β luciferase reporter construct were gifts from Dr. Kate Fitzgerald (University of Massachusetts Medical School, Worchester, MA). The PRDII, PRDI-III, and PRDIV luciferase reporter constructs were gifts from Dr. Sinead Miggin (National University of Ireland, Maynooth, Ireland). pcDNAPPARα and the reporter plasmid 3xPPRE TK-luc were kind gifts from Dr. Andrew Bennett (University of Nottingham, UK). *R(+)*WIN55,212-2, *S(−)*WIN55,212-2, the PPARα agonist fenofibrate, the selective JNK inhibitor SP600125 (all from Sigma), and the PPARα antagonist GW6471 (Tocris Bioscience, Bristol, UK) were initially dissolved in DMSO and stored as 10 mM stock solutions. For culture use, the stock drugs were diluted to a final concentration in culture medium, and DMSO (<0.1%) was used as a vehicle control. Human embryonic kidney 293 (HEK293) cells stably expressing the TLR3 receptor were from InvivoGen (Toulouse, France).

Cell Culture—Cell lines were maintained in DMEM supplemented with 10% FBS, 100 μg/ml penicillin, and 100 μg/ml streptomycin. Cells were maintained in a 37 °C humidified atmosphere with 5% CO_2. The neomycin analog G418 (500 μg/ml) was used to select for the stably transfected TLR cell lines and maintenance of CD14 expression. Primary astrocytes were prepared as described previously (27) from the whole brain of 1-day-old C57/BL6 mice in accordance with the guidelines laid down by the local ethics committee (National University of Ireland Maynooth). Briefly, dissected brains were chopped, added to DMEM (Invitrogen), triturated, passed through a sterile mesh filter (40 μm), and centrifuged (2,000 × *g* for 3 min at 20 °C). The pellet was resuspended in DMEM and plated onto T25 flasks. Medium was changed after 1, 5, and 8 days. Astrocytes were isolated from mixed glia at day 10–14 by removing non-adherent cells with mechanical shaking and harvesting by trypsinization (0.25% trypsin, 0.02% EDTA). Cells were centrifuged (2,000 × *g* for 5 min at 20 °C), and the astrocyte-enriched pellet was resuspended in DMEM. Astrocytes were plated (2 × 10^5 cells/ml) on 6- or 12-well plates and treated 24 h later.

Transient Transfections—HEK293 cells (2 × 10^5 cells/ml) were seeded in 96-well plates and allowed to adhere for 24 h. Cells were transfected using Lipofectamine 2000 with firefly luciferase NF-κB reporter plasmids (80 ng); constitutively expressed *Renilla* luciferase reporter constructs (phRL-TK) (20 ng); IFN-β luciferase reporter constructs (80 ng); AP-1 luciferase reporter constructs (80 ng); PRDII, PRDI-III, and PRDIV luciferase reporter constructs (80 ng); and expression constructs encoding mitogen-activated protein kinase kinase kinase (MEKK1) (20 ng). Total DNA was kept constant using the pcDNA3.1 empty vector. To measure the activation of Jun and IRF3, cells were transfected with pFR-Luc (60 ng) and the *trans*-activator plasmids pFA-Jun (Jun fused downstream of the yeast Gal4 DNA binding domain, 30 ng) and pFA-IRF3 (IRF3 fused downstream of the yeast Gal4 DNA binding domain, 30 ng). For PPARα luciferase reporter gene assays, HEK293 cells were transiently transfected with pcDNAPPARα (500 ng) together with the reporter plasmid 3xPPRE TK-luc (1 μg). Cells were allowed to recover overnight and then pretreated with/ without GW6471 (1 μM; 1 h) or SP600125 (10 μM; 1 h) prior to exposure to *R(+)*WIN55,212-2 (0.001–40 μM), *S(−)*-

WIN55,212-2 (20 μM) or fenofibrate (0.001–40 μM) for 1 h (overnight treatment to assess PPARα transactivation as based on previous observations) (13). The inhibitor concentrations were selected based on the IC$_{50}$ values for antagonism in cell-based assays (28–29). The concentrations of *R*(+)-WIN55,212-2 used are in line with those used in various anti-inflammatory paradigms *in vitro* (30–32). Furthermore, the concentrations of fenofibrate tested were based on the EC$_{50}$ values of the compound in transactivation assays (33). Cells were then stimulated in the presence or absence of the TLR3 ligand, poly(I:C) (25 μg/ml; InvivoGen) for a further 6 h (time point was selected based on previous evidence) (34). Cell extracts were generated using reporter lysis buffer (Promega, Southampton, UK), and extracts were assayed for firefly luciferase and *Renilla* luciferase activity using the Luciferase assay system (Promega) and coelenterazine (1 μg/ml), respectively. Luminescence was monitored with a Glomax microplate luminometer (Promega). The *Renilla* luciferase plasmid was used to normalize for transfection efficiency in all experiments.

ELISA—Primary astrocytes (2 × 10^5 cells/ml) were seeded in 12-well plates. Cells were pretreated with or without GW6471 (1 μM; 1 h) prior to *R*(+)WIN55,212-2 (20 μM; 1-h pretreatment). Cells were then treated with poly(I:C) (25 μg/ml) for 6 h. Cell culture supernatants were assayed for levels of RANTES by ELISA according to the manufacturer's instructions (Duoset, R&D Systems, Abingdon, UK).

Western Blotting—Astrocytes were seeded in 6-well plates (2 × 10^5 cells/ml). Cells were treated with *R*(+)WIN55,212-2 (20 μM), fenofibrate (20 μM) (time points ranging from 5 min to 24 h), and *S*(−)WIN55,212-2 (20 μM; 8 h) or pretreated with or without GW6471 (1 μM; 1 h) prior to *R*(+)WIN55,212-2 (20 μM; 15 min). Cells were then washed in ice-cold PBS before being lysed on ice for 10 min in 150 μl of lysis buffer (20 mM HEPES, pH 7.4, containing 10 mM KCl, 1.5 mM MgCl$_2$, 1 mM EDTA, 1 mM EGTA, 1 mM dithiothreitol, 0.1 mM PMSF, 0.5% Igepal, pepstatin A (5 μg/ml), leupeptin (2 μg/ml), and aprotinin (2 μg/ml)). Cell lysates were centrifuged at 13,000 × *g* for 15 min at 4 °C. The supernatant was mixed with SDS-PAGE sample buffer (0.125 Tris-HCl, pH 6.8, 20% (v/v) glycerol, 4% (w/v) SDS, 1.4 M β-mercaptoethanol, and 0.0025% (w/v) bromphenol blue). Samples were boiled (10 min) and separated on 10% SDS-polyacrylamide gels, and proteins were transferred to nitrocellulose membrane (Sigma). Membranes were blocked for 1 h in 5% BSA. Membranes were incubated overnight at 4 °C with rabbit polyclonal phospho-JNK (1:1,000 in 5% BSA), goat polyclonal PPARα (1:1,000 in 5% dried milk), and rabbit polyclonal total JNK antibody (1:1,000 in 5% BSA). Membranes were washed and incubated with anti-goat or anti-rabbit IRDye Infrared secondary antibody (1:5,000 in 5% dried milk; LI-COR Biosciences, Lincoln, NE) for 1 h in the dark at room temperature. The membranes were then washed, and immunoreactive bands were detected using the Odyssey Infrared Imaging System (LI-COR Biosciences). Membranes were stripped and incubated with mouse monoclonal anti-β-actin antibody (1:10,000; overnight at 4 °C; Sigma). Molecular weight markers were used to calculate molecular weights of proteins represented by immunoreactive bands. Densitometry was per-

formed using ImageJ software, and values were normalized for protein loading relative to levels of total JNK or β-actin.

Quantitative RT-PCR—HEK293 cells and primary astrocytes (both at 2 × 10^5 cells/ml) were seeded on 6-well plates. Cells were pretreated with or without the PPARα antagonist GW6471 (1 μM; 1 h) prior to exposure to *R*(+)WIN55,212-2 (20 μM; 1 h). In some experiments, cells were pretreated with or without fenofibrate (1–40 μM; 1 h). Cells were then treated in the absence or presence of poly(I:C) (25 μg/ml) for 4 h. In another series of experiments, primary astrocytes were treated with *R*(+)WIN55,212-2 (20 μM) or *S*(−)WIN55,212-2 (20 μM) for times ranging from 1 to 24 h. RNA was extracted from cells using Tri Reagent™ (Invitrogen), and cDNA was generated from normalized RNA using Superscript II reverse transcriptase. cDNA (1 μg) was amplified in the presence of SYBR® Green PCR Mastermix (New England Biolabs, Ipswich, MA). Primers used were as follows: murine IFN-β, forward (5′-GGAGATGACGGAGAAGATGC-3′) and reverse (5′-CCCAGTGCTGGAGAAATTGT-3′); murine PPARα, forward (5′-CCTCAGGGTACCACTACGGAGT-3′) and reverse (5′-GCCGAATAGTTCGCCGAA-3′); human IFN-β, forward (5′-GACCAACAAGTGTCTCCTCCAAA-3′) and reverse (5′-CTCCTCAGGGATGTCAAAGTTCA-3′). As internal control, murine GAPDH (forward, 5′-AGGTCATCCCAGAGCT-GAACG-3′; reverse, 5′-ACCCTGTTGCTGTAGCCGTA-3′) and human HPRT (forward, 5′-TTGCTGACCTGCTGGAT-TAC-3′; reverse, 5′-TCTCCACCAATTACTTTTATGTCC-3′) were used in a similar reaction. Accumulation of gene-specific PCR products was measured continuously by means of fluorescence detection over 40 cycles. Samples were run in duplicate as follows: 10 min at 95 °C and for each cycle, 10 s at 95 °C, 10 s at 55 °C, and 1 min at 72 °C. Gene expression was calculated relative to the endogenous control, and analysis was performed using the $2^{-\Delta\Delta C_T}$ method.

Confocal Microscopic Analysis of PPARα—Primary astrocytes were seeded (1 × 10^5 cells/ml) in 4-well chamber slides (Lab-Tek, Roskilde, Denmark) and grown for 24 h. Cells were treated with *R*(+)WIN55,212-2 (20 μM) or *S*(−)WIN55,212-2 (20 μM) for times ranging from 2 to 8 h. Cells were fixed in 4% paraformaldehyde and blocked with 10% chicken serum (Vector Laboratories, Peterborough, UK) for 2 h. Cells were treated overnight at 4 °C with goat polyclonal PPARα antibody (1:100 in 5% chicken serum; Santa Cruz Biotechnology, Inc., Santa Cruz, CA). Cells were washed and incubated with chicken anti-goat Alexa488 secondary antibody (1:500 in 5% chicken serum; Invitrogen) and DAPI (1.5 μg/ml) in PBS, washed, and mounted (Vectashield, Vector Laboratories). All samples were viewed using an Olympus FluoView FV1000 confocal laser-scanning microscope equipped with the appropriate filter sets. Acquired images were analyzed using the Olympus FV-10 ASW imaging software. Negative control experiments were performed by replacing the primary antibody with isotype control IgG (Millipore, Cork, Ireland) and using equal gain settings during acquisition and analysis.

Induction and Assessment of EAE and Treatment with Cannabinoid and PPARα Antagonist—EAE was induced in mice as described (35). Female SJL/J mice (10 weeks old) were injected subcutaneously at two sites with two injections (100 μl) of
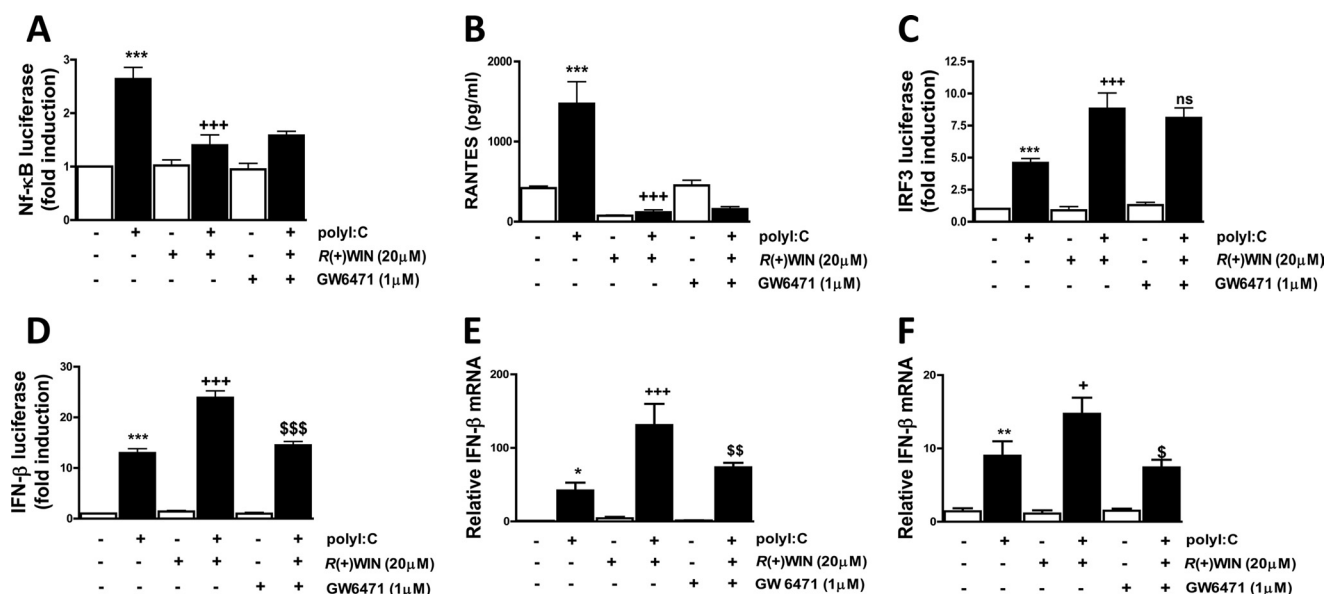
FIGURE 1. **R(+)WIN55,212-2 acts via PPARα to potentiate TLR3-induced IFN-β expression.** *A*, HEK293-TLR3 cells were co-transfected with plasmids encoding NF-κB-regulated firefly luciferase and TK *Renilla* luciferase. 24 h post-transfection, cells were treated in the absence or presence of GW6471 (1 μM) prior to *R*(+)WIN55,212-2 (20 μM) for 1 h. Cells were then treated with or without poly(I:C) (25 μg/ml) for 6 h. Lysates were assayed for luciferase activity and normalized for transfection efficiency using *Renilla* luciferase activity. *B*, primary mouse astrocytes were pretreated with GW6471 (1 μM; 1 h) prior to *R*(+)WIN55,212-2 (20 μM; 1 h) and poly(I:C) (25 μg/ml) exposure. Supernatants were analyzed for RANTES production using ELISA. *C*, HEK293-TLR3 cells were co-transfected with pFA-IRF3 and pFR-regulated firefly luciferase and TK *Renilla* luciferase. Transfected cells were left overnight and treated in the absence or presence of GW6471 (1 μM) prior to *R*(+)WIN55,212-2 (20 μM) for 1 h. Cells were then treated with or without poly(I:C) (25 μg/ml) for 6 h, and lysates were assayed for luciferase activity. *ns*, not significant. *D*, HEK293-TLR3 cells were co-transfected with IFN-β promoter-regulated firefly luciferase and TK *Renilla* luciferase, left overnight, and treated in the absence or presence of GW6471 (1 μM; 1 h) prior to *R*(+)WIN55,212-2 (20 μM; 1 h) and poly(I:C) (25 μg/ml) exposure for 6 h. Lysates were assayed for luciferase activity. Primary astrocytes (*E*) and HEK293-TLR3 (*F*) were pretreated with GW6471 (1 μM; 1 h) prior to *R*(+)WIN55,212-2 (20 μM; 1 h) and poly(I:C) (25 μg/ml) exposure for 6 h. cDNA was generated and assayed by quantitative real-time PCR for levels of IFN-β mRNA. The expression level of IFN-β was normalized relative to expression of the housekeeping gene GAPDH or HPRT. Data are presented as the mean ± S.E. (*error bars*) of triplicate determinations and are representative of three independent experiments (*A*, *C*, *D*, and *F*) or are triplicate determinations from six animals (*B* and *E*). *, $p < 0.05$; **, $p < 0.01$; ***, $p < 0.001$ compared with vehicle-treated cells. +, $p < 0.05$; +++, $p < 0.001$ compared with poly(I:C)-treated cells. \$, $p < 0.05$; \$\$, $p < 0.01$; \$\$\$, $p < 0.001$ compared with cells treated with poly(I:C) in the presence of *R*(+)WIN55,212-2.

emulsified Freund's complete adjuvant containing 100 μg of myelin proteolipid protein amino acids 139–151 (PLP(139–151)) and 200 μg of *Mycobacterium tuberculosis* H37Ra followed 2 h later with 200 ng of pertussis toxin (Hooke Laboratories, Lawrence, MA) delivered intraperitoneally. *R*(+)WIN55,212-2 was prepared in Cremophor El (Sigma) and PBS (20:80) and administered (20 mg/kg) intraperitoneally on days 0, 1, 2, 3, 4, and 5. The preparation and immunization of the synthetic cannabinoid *R*(+)WIN55,212-2 (Sigma) was modified from previous studies (36). GW6471 was dissolved in DMSO and administered intraperitoneally (10 mg/kg) on days 0, 1, 2, 4, and 6 after PLP immunization. Control mice received Cremophor/PBS (20:80) as vehicle. Data are from 4–8 mice/group. To ensure objective clinical scoring, all mice had electronic data chips placed subcutaneously prior to the experiment and were subsequently tracked by a barcode reader (AVID, UK). An investigator blinded to the treatment of the mice scored all animals by barcode number, to determine the mean clinical score as follows: 0, normal; 1, limp tail or hind limb weakness; 2, limp tail and hind limb weakness, 3, partial hind limb paralysis; 4, complete hind limb paralysis; 5, moribund.

Statistical Analysis—Data are expressed as means with S.E., and the results represent three independent experiments. Statistical comparisons of different treatments were done by a one-way analysis of variance using a post hoc Student-Newman-Keuls test. Differences with a *p* value less than 0.05 were considered statistically significant.

RESULTS

R(+)WIN55,212-2 Enhances TLR3-induced IFN-β Expression via PPARα—We have previously demonstrated that *R*(+)WIN55,212-2 negatively regulates the transactivation of NF-κB and expression of proinflammatory cytokines (37) but can positively impact the TLR3-IRF3 signaling axis to enhance IFN-β expression in the presence of TLR3 stimulation (8). Given that such effects were shown to be mediated in a manner independent of cannabinoid receptors (8, 37) and that this compound can exert some effects via PPARα (13, 38), we used the specific PPARα antagonist GW6471 to assess the potential role of PPARα in mediating the effects of *R*(+)WIN55,212-2 on TLR3-induced activation of NF-κB and IRF3 and expression of TLR-responsive genes. GW6471 failed to regulate the ability of *R*(+)WIN55,212-2 to inhibit TLR3-induced activation of NF-κB in HEK293-TLR3 cells (Fig. 1A) or the expression of the NF-κB-responsive chemokine RANTES in astrocytes (Fig. 1B), indicating that these effects of *R*(+)WIN55,212-2 are mediated in a manner independent of PPARα. Similarly, the potentiating effect of *R*(+)WIN55,212-2 on TLR3-induced IRF3 activation in HEK293-TLR3 cells was not reliant on the PPARα isoform, given that GW6471 failed to influence the effects of *R*(+)WIN55,212-2 on IRF3 activation (Fig. 1C). The lack of a
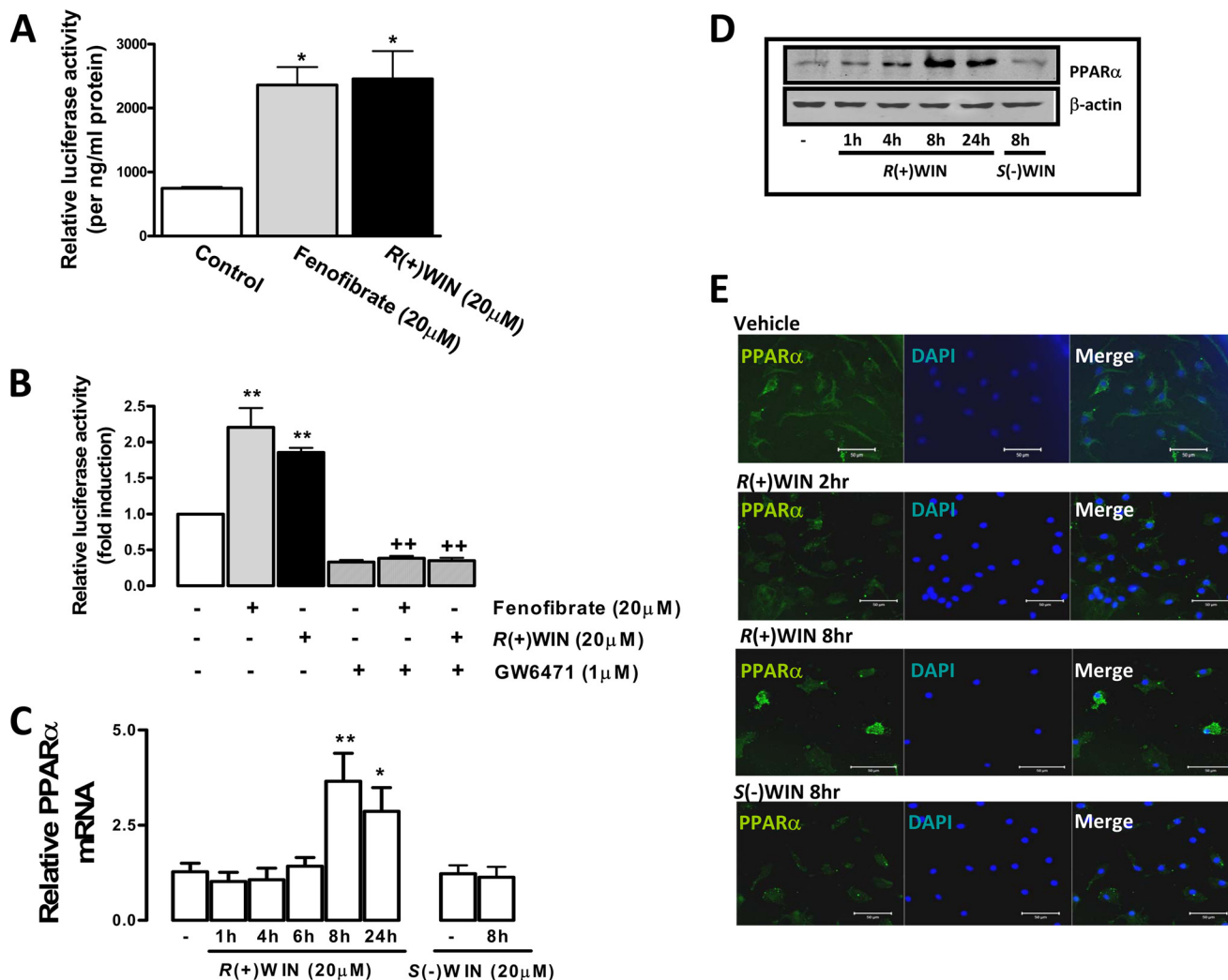
FIGURE 2. **The effects of *R(+)*WIN55,212-2 on PPARα-mediated transcriptional activity and expression.** *A* and *B*, HEK293 cells were co-transfected with PPARα and PPRE-luc reporter constructs; *B*, preincubated with GW6471 (1 μM; 1 h) prior to treatment overnight with *R(+)*WIN55,212-2 (20 μM) and fenofibrate (20 μM). Lysates were assayed for firefly luciferase activity and normalized to protein concentration. *C*, primary astrocytes and were treated with *R(+)*WIN55,212-2 (20 μM; 1–24 h) or *S(−)*WIN55,212-2 (20 μM; 8 h). cDNA was generated and assayed by quantitative real-time PCR for levels of PPARα mRNA. The expression level of PPARα was normalized relative to expression of GAPDH. *D*, primary astrocytes were treated with *R(+)*WIN55,212-2 (20 μM; 1–24 h) or *S(−)*WIN55,212-2 (20 μM; 8 h). Cell lysates were prepared and subsequently subjected to Western immunoblotting using anti-PPARα and anti-β-actin antibodies. *E*, primary astrocytes were grown in chamber slides and treated with *R(+)*WIN55,212-2 (20 μM; 2– 8 h) or *S(−)*WIN55,212-2 (20 μM; 8 h). Cells were fixed, mounted in anti-fade medium with DAPI, and visualized using confocal microscopy. Confocal images were captured using a UV Zeiss 510 Meta System laser-scanning microscope equipped with the appropriate filter sets. Images are representative of three independent experiments. *Scale bars*, 20 μm. Data are mean ± S.E. (*error bars*) of triplicate determinations and are representative of three independent experiments (*A* and *B*) or are representative of data obtained from 6–9 animals (*C* and *D*). *, $p < 0.05$; **, $p < 0.01$ compared with vehicle-treated cells. ++, $p < 0.01$ compared with cells treated with fenofibrate and *R(+)*WIN55,212-2.

role for PPARα in regulating IRF3 was further confirmed in HEK293 cells by demonstrating that GW6471 failed to regulate the previously described ability of *R(+)*WIN55,212-2 to promote the increased nuclear localization of IRF3-GFP fusion protein (supplemental Fig. 1). However, pre-exposure to the PPARα antagonist GW6471 attenuated the ability of *R(+)*WIN55,212-2 to enhance poly(I:C)-induced activation of the IFN-β promoter (Fig. 1*D*) and to potentiate poly(I:C)-induced IFN-β mRNA expression in primary astrocytes (Fig. 1*E*) and HEK293-TLR3 cells (Fig. 1*F*), indicating that *R(+)*WIN55,212-2 enhances TLR3-induced IFN-β expression via a PPARα mechanism.

R(+)WIN55,212-2 Promotes Increased Transactivation and Expression of PPARα—Because *R(+)*WIN55,212-2 enhances IFN-β expression via a PPARα mechanism, we next assessed

the potential of *R(+)*WIN55,212-2 to directly regulate the activation and expression of PPARα. *R(+)*WIN55,212-2 was initially compared with the PPARα-specific agonist fenofibrate for its ability to transactivate PPARα and increase the expression of a luciferase reporter gene that is regulated by a PPARα-responsive element. Fenofibrate and *R(+)*WIN55,212-2 demonstrated a significant increase in PPARα-mediated transcription in HEK293 cells (Fig. 2*A*) with both agents directly acting on PPARα because their effects were abrogated by the PPARα antagonist GW6471 (Fig. 2*B*). Furthermore, exposure of primary astrocytes to *R(+)*WIN55,212-2 significantly enhanced the expression of PPARα mRNA in a time-dependent manner, with mean maximal stimulatory effects observed at 8–24 h post-aminoalkylindole exposure (Fig. 2*C*). The stimulatory effect of *R(+)*WIN55,212-2 on PPAR expression was restricted
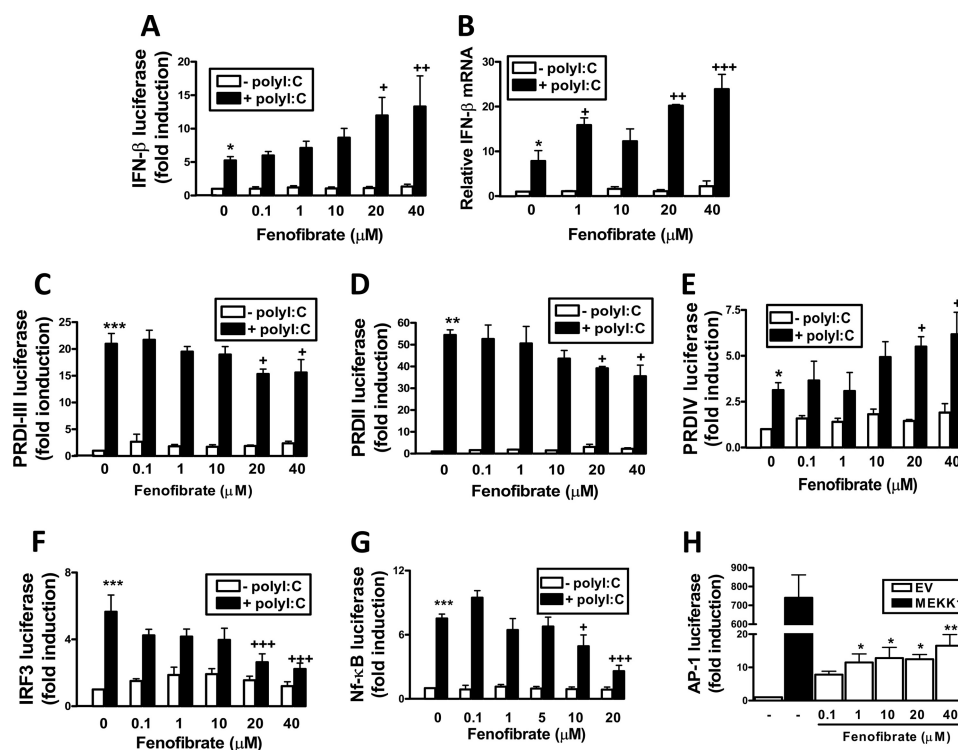
FIGURE 3. **Fenofibrate targets PRDIV.** HEK293-TLR3 cells were co-transfected with IFN-β promoter-regulated firefly luciferase (*A*), PRDI-III (*C*), PRDII (*D*), PRDIV (*E*), pFA-IRF3- and pFR-regulated firefly luciferase (*F*), and NF-κB-regulated firefly luciferase (*G*) in addition to TK *Renilla* luciferase. Cells were left overnight and pretreated in the absence or presence of fenofibrate (0.1–40 μM; 1 h) and stimulated with poly(I:C) (25 μg/ml) for 6 h. Lysates were assayed for luciferase activity. *B*, HEK293-TLR3 were pretreated with fenofibrate (1–40 μM; 1 h) prior to poly(I:C) (25 μg/ml) exposure for 6 h. cDNA was generated and assayed by quantitative real-time PCR for levels of IFN-β mRNA. The expression level of IFN-β was normalized relative to expression of HPRT. *H*, HEK293-TLR3 cells were co-transfected with AP-1 luciferase reporter construct and TK *Renilla* luciferase with or without a construct encoding MEKK1. Empty vector pcDNA3.1 (*EV*) was used to normalize the amount of total DNA transfected. Cells were treated with fenofibrate (0.1–40 μM) for 6 h. Lysates were assayed for luciferase activity. Data are presented as the mean ± S.E. (*error bars*) of triplicate determinations and are representative of three independent experiments. *, $p < 0.05$; **, $p < 0.01$; ***, $p < 0.001$ compared with vehicle-treated cells. +, $p < 0.05$; ++, $p < 0.01$; +++, $p < 0.001$ compared with poly(I:C)-treated cells.

to the α isoform because it had no effect on PPARδ or PPARγ mRNA expression in astrocytes (data not shown). The enantiomeric form of $R(+)$WIN55,212-2, $S(-)$WIN55,212-2 (39), failed to affect PPARα mRNA expression (Fig. 2*C*), suggesting that a stereoselective mechanism underlies the stimulatory effects of $R(+)$WIN55,212-2 on PPARα. The time- and stereoselective-dependent effects of $R(+)$WIN55,212-2 on PPARα expression were also confirmed at the protein level by immunoblotting of extracts from $R(+)$WIN55,212-2-treated astrocytes (Fig. 2*D*). We also employed confocal microscopy to characterize the effects of $R(+)$WIN55,212-2 on the cellular expression pattern and localization of PPARα. Exposure of astrocytes to $R(+)$WIN55,212-2 promoted strong cellular expression of PPARα from 8 h, and this was highly localized to the nucleus (Fig. 2*E*). These findings strongly indicate that $R(+)$WIN55,212-2 positively regulates the activation and expression of PPARα, and this is consistent with the PPARα dependence of $R(+)$WIN55,212-2 with respect to its regulatory effects on IFN-β.

PPARα Targets the PRDIV Domain of the IFN-β Promoter— Given that $R(+)$WIN55,212-2 can directly target PPARα and augment TLR3-induced activation of the IFN-β promoter in a PPARα-dependent manner, we next examined if activation of PPARα was sufficient to manifest such positive effects. We thus examined the ability of the PPARα-specific agonist fenofibrate to regulate activation of the IFN-β promoter. Fenofibrate aug-

mented poly(I:C)-induced activation of the IFN-β promoter (Fig. 3*A*) and induction of IFN-β mRNA (Fig. 3*B*) in a dose-dependent manner in HEK293-TLR3 cells, indicating that activation of PPARα is indeed sufficient to positively regulate IFN-β. We next probed the mechanistic basis to the regulatory effects of PPARα on the IFN-β promoter. Transcriptional activation of IFN-β requires assembly of a transcription enhancer complex on the four PRDs of its promoter. PRDI-III domains are recognized by IRF3/7, PRDII is recognized by NF-κB, and PRDIV is recognized by AP-1 (7). We thus assessed the regulatory influence of PPARα on each of these regulatory regions by measuring the effects of fenofibrate on poly(I:C) induction of a luciferase reporter gene regulated by individual PRDs. Fenofibrate, in a dose-dependent manner, inhibited poly(I:C)-induced activation of PRDI-III (Fig. 3*C*) and PRDII (Fig. 3*D*) but intriguingly augmented poly(I:C)-induced activation of PRDIV (Fig. 3*E*). Fenofibrate had no effect on cell viability (supplemental Fig. 2) at the concentrations tested. We next probed the direct effects of fenofibrate on the transcription factors that bind to each of the PRD regions. Fenofibrate, in a dose-dependent manner, inhibited poly(I:C)-induced IRF3-regulated luciferase (Fig. 3*F*), and this is consistent with the negative effects of fenofibrate on PRDI-III. Fenofibrate also showed strong inhibitory effects on poly(I:C)-induced activation of NF-κB (Fig. 3*G*), and this provides a credible basis to the negative effects of fenofibrate on PRDII. Interestingly, fenofibrate induced activation of AP-1
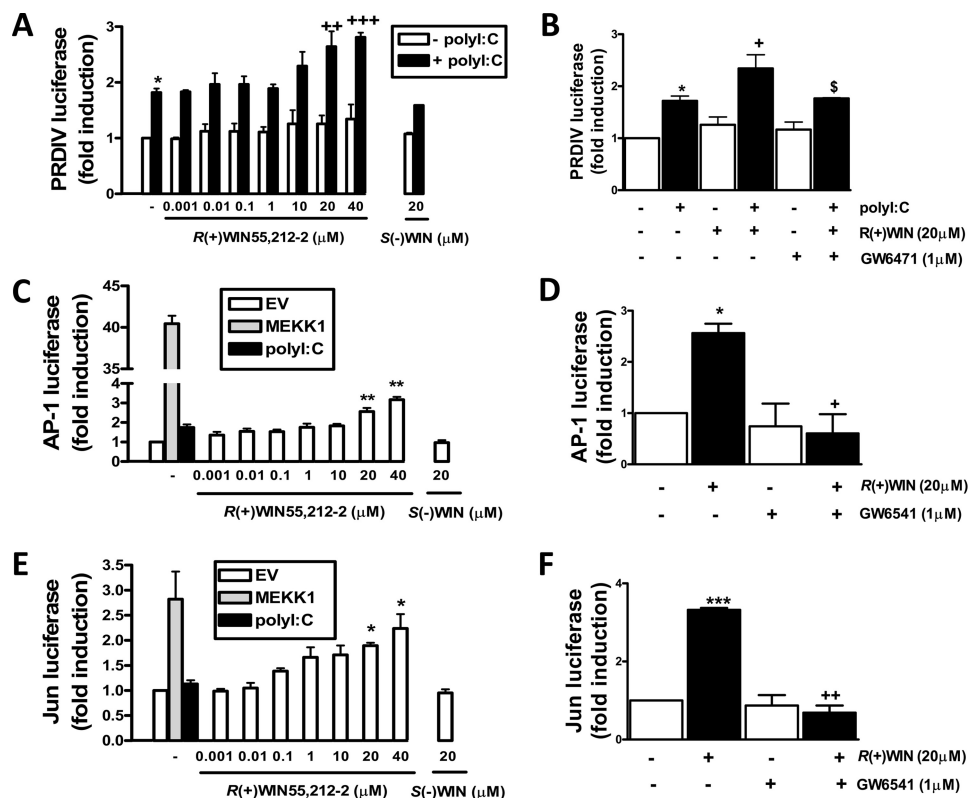
FIGURE 4. R(+)WIN55,212-2 acts via PPARα to target PRDIV, AP-1, and Jun transcription factors. HEK293-TLR3 cells were co-transfected with PRDIV (*A and B*), AP-1 luciferase reporter construct (*C and D*), and pFR-Luc (*E and F*) and the *trans*-activator plasmid pFA-Jun in addition to constitutively expressed TK *Renilla* luciferase. Cells were left overnight and treated with or without R(+)WIN55,212-2 (0.001–40 μM; 1 h) or S(−)WIN55,212-2 (20 μM; 1 h) prior to poly(I:C) (25 μg/ml; 6 h) exposure (*A, C, and E*) or pretreated with GW6471 (1 μM; 1 h) prior to R(+)WIN55,212-2 (20 μM; 6 h) and subsequent poly(I:C) (25 μg/ml; 6 h) (*B*) exposure (*B, D, and F*). *C and E*, cells were also treated with a construct encoding MEKK1, and empty vector pcDNA3.1 (*EV*) was used to normalized the amount of total DNA transfected. Lysates were assayed for luciferase activity. Data are presented as the mean ± S.E. (*error bars*) of triplicate determinations and are representative of three independent experiments. *, $p < 0.05$; **, $p < 0.01$; ***, $p < 0.001$ compared with vehicle-treated cells. +, $p < 0.05$; ++, $p < 0.01$; +++, $p < 0.001$ compared with poly(I:C)-treated (*A and B*) or R(+)WIN55,212-2-treated cells (*D and F*). $, $p < 0.05$ compared with cells treated with poly(I:C) in the presence of R(+)WIN55,212-2.

(Fig. 3*H*), and this is consistent with the positive effects of fenofibrate on PRDIV.

R(+)WIN55,212-2 Targets the PRDIV Domain of the IFN-β Promoter by Activating AP-1 in a PPARα-dependent Manner— The positive regulatory effects of fenofibrate on the PRDIV region of the IFN-β promoter, coupled to the PPARα-mediated activation of the IFN-β promoter by R(+)WIN55,212-2, prompted an assessment of the regulatory effects of the latter on the PRDIV domain. Similar to fenofibrate, R(+)WIN55,212-2 augmented poly(I:C)-induced activation of PRDIV luciferase in HEK293-TLR3 cells in a dose-dependent and stereoselective manner (Fig. 4A). This effect was blocked by the PPARα antagonist GW6471 (Fig. 4*B*), indicating that R(+)WIN55,212-2 targets PRDIV via PPARα and so regulates TLR3-induced activation of the IFN-β promoter. Given that AP-1 targets PRDIV, we next assessed the impact of R(+)WIN55,212-2 on activation of AP-1. Poly(I:C) proved to be a very weak activator of AP-1, but R(+)WIN55,212-2 caused a dose-dependent induction of the AP-1-regulated luciferase gene (Fig. 4*C*). The stimulatory effect of R(+)WIN55,212-2 on the latter was mediated by PPARα because pre-exposure to GW6471 precluded R(+)WIN55,212-2-induced activation of AP-1 (Fig. 4*D*). In order to further probe the mechanism by which R(+)WIN55,212-2 activates AP-1, we assessed its ability to activate Jun, a major transactivating subunit of AP-1.

HEK293 cells were thus transfected with a construct encoding a fusion protein of Jun and the DNA binding domain of the yeast protein Gal4 and a luciferase reporter construct regulated by a promoter containing a Gal4 binding motif. R(+)WIN55,212-2 induced the transactivation of the Jun-Gal4 protein in a dose-dependent and stereoselective manner (Fig. 4*E*) and by a mechanism that is dependent on PPARα because the positive effects of R(+)WIN55,212-2 were abrogated by GW6471 (Fig. 4*F*).

R(+)WIN55,212-2 Promotes JNK Phosphorylation and JNK Mediates the Effects of R(+)WIN55,212-2 on the IFN-β Promoter— Given that R(+)WIN55,212-2 targets activation of Jun in a PPARα-dependent manner, we next examined the regulatory effects of R(+)WIN55,212-2 and fenofibrate on activation of JNK, the immediate upstream kinase of Jun (40). Dual phosphorylation of closely positioned threonine and tyrosine residues in JNK is commonly used as an index of JNK activation, and we employed phosphospecific antibodies to characterize the effects of the above ligands on JNK activation. R(+)-WIN55,212-2 promoted a time-dependent increase in JNK phosphorylation in astrocytes (Fig. 5A), and this was also observed in response to fenofibrate (Fig. 5B). GW6471 prevented R(+)WIN55,212-2-induced JNK phosphorylation (Fig. 5C), demonstrating that the activation of JNK by R(+)WIN55,212-2 is PPARα-dependent. In addition, the JNK inhibitor SP600125 significantly inhibited the stimulatory
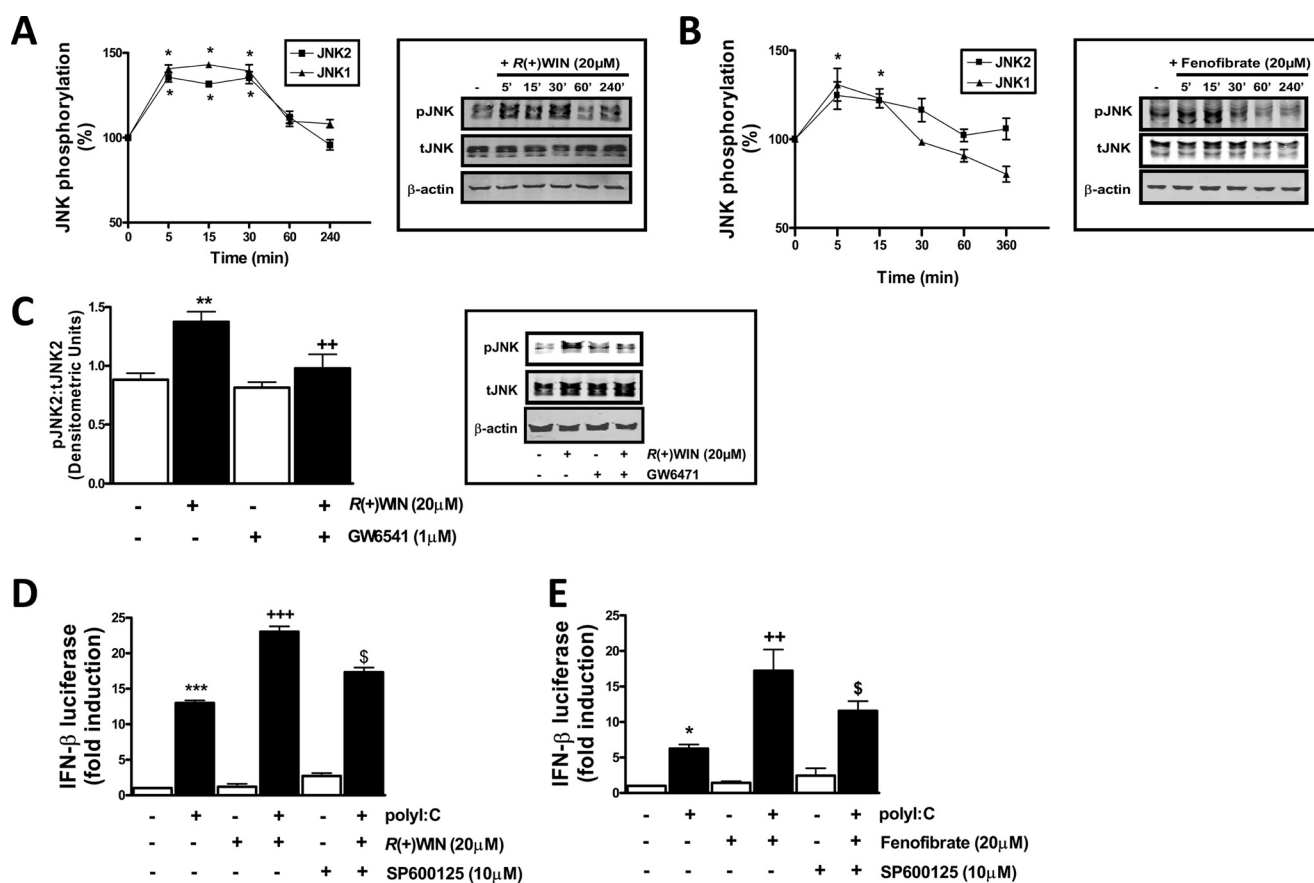
FIGURE 5. **R(+)WIN55,212-2 targets JNK to promote IFN-β expression.** *A* and *B*, primary mouse astrocytes were seeded into 6-well plates and treated with *R*(+)WIN55,212-2 (20 μM) (*A*) or fenofibrate (20 μM) (*B*) for various times (5–240 min). Cell lysates were subsequently subjected to Western immunoblotting using anti-phospho-JNK, anti-total JNK, and anti-β-actin antibodies. *C*, primary astrocytes were treated with GW6471 (1 μM; 1 h) prior to *R*(+)WIN55,212-2 (20 μM) for 15 min, and lysates were prepared and subjected to immunoblotting. All immunoblots were subjected to densitometric analysis with levels of phospho-JNK normalized to total levels of JNK. *D* and *E*, HEK293-TLR3 cells were co-transfected with IFN-β promoter-regulated firefly luciferase and TK *Renilla* luciferase, left overnight, and pretreated (1 h) with SP600125 (10 μM) in the absence or presence of *R*(+)WIN55,212-2 (20 μM) (*D*) or fenofibrate (20 μM) (*E*) prior to poly(I:C) (25 μg/ml) for 6 h. Lysates were assayed for firefly luciferase activity. Data are mean ± S.E. (*error bars*) of triplicate determinations and are representative of three independent experiments (*D* and *E*) or represent densitometric data from 5–9 animals (*A–C*). *, $p < 0.05$; **, $p < 0.01$; ***, $p < 0.001$ compared with vehicle-treated cells. +, $p < 0.05$; ++, $p < 0.01$; +++, $p < 0.001$ compared with *R*(+)WIN55,212-2-treated cells (*C*) or poly(I:C)-treated cells (*D* and *E*). $, $p < 0.05$ compared with cells treated with poly(I:C) in the presence of *R*(+)WIN55,212-2 or fenofibrate.

effect of *R*(+)WIN55,212-2 (Fig. 5*D*) and fenofibrate (Fig. 5*E*) on TLR3-induced activation of the IFN-β promoter, indicating that activation of JNK by *R*(+)WIN55,212-2 and PPARα is a critical step mediating the positive effects of the synthetic cannabinoid on activation of the IFN-β promoter.

Treatment with GW6471 Ameliorates the Protective Effects of R(+)WIN55,212-2 in EAE during the First Paralytic Episode— Our laboratory (8) and others (41) have previously demonstrated protective effects of *R*(+)WIN55,212-2 in EAE. Importantly, the neuroprotective effects of *R*(+)WIN55,212-2 in EAE are IFN-β-dependent (8). Given that data herein demonstrate that *R*(+)WIN55,212-2 regulates TLR3-induced IFN-β expression via PPARα, we assessed the role of this receptor in mediating the effects of *R*(+)WIN55,212-2 in a relapsing mouse model of EAE involving immunization with PLP(139–151). PLP-immunized mice developed clinical symptoms of disease 11–14 days postimmunization, with partial recovery observed within 7 days (Fig. 6). From 22 to 30 days postimmunization, mice developed a second wave of paralysis, indicative of relapse (Fig. 6). Mice treated with *R*(+)WIN55,212-2 showed significantly reduced severity of EAE during both the first (14–18

days postimmunization) and second (24–26 days and 28–30 days postimmunization) paralytic episodes. However, PLP-immunized mice treated with *R*(+)WIN55,212-2 in the presence of GW6471 showed significantly reduced protection during the first (days 15, 16, and 18 postimmunization) paralytic episode (Fig. 6), indicating that the effects of *R*(+)WIN55,212-2 display some PPARα dependence during this phase of the disease. Animals that received GW6471 alone displayed a similar disease course as control animals throughout the experiment.

DISCUSSION

This study defines a non-cannabinoid-dependent mechanism of action for the aminoalkylindole *R*(+)WIN55,212-2, in that this synthetic cannabinoid receptor agonist regulates IFN-β expression via the PPARα nuclear receptor. In so doing, the study also highlights the highly novel role of PPARα in regulating IFN-β expression. Previously, we have demonstrated that *R*(+)WIN55,212-2 augments TLR3 signaling to IRF3 activation and IFN-β expression, and this contributes to the therapeutic effects of *R*(+)WIN55,212-2 in animal models of MS (8). Here, we now demonstrate that *R*(+)WIN55,212-2 also
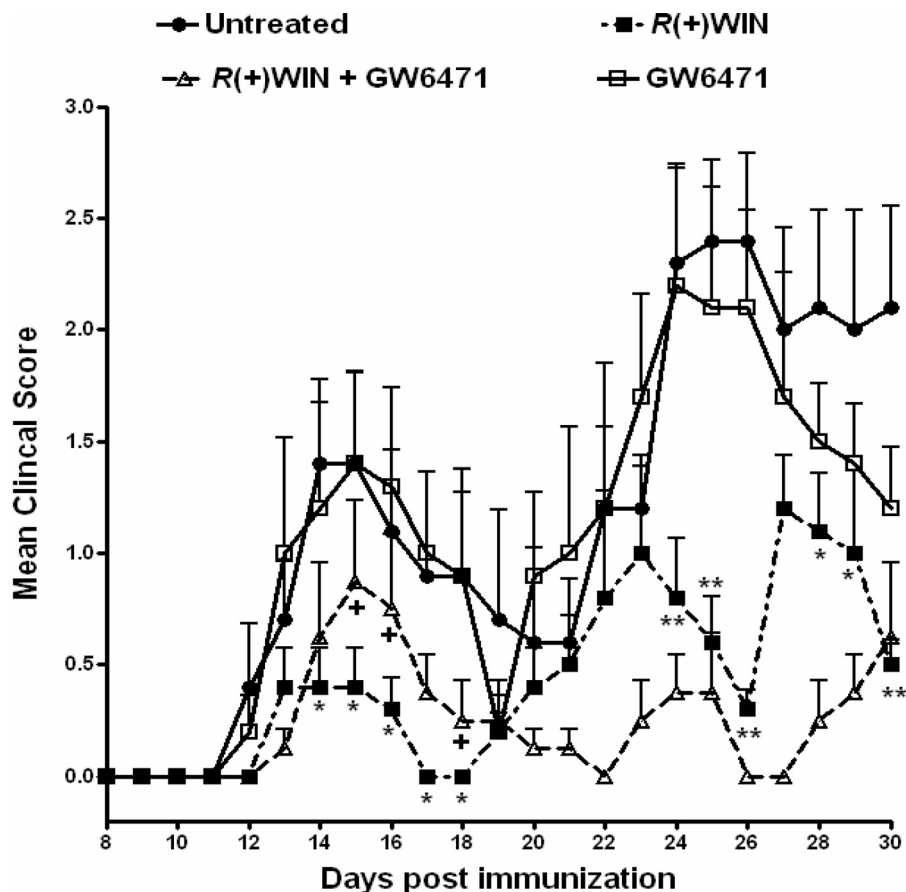
FIGURE 6. **PPARα contributes to the protective effects of R(+)WIN55,212-2 in EAE.** Female SJL/J mice were injected with emulsified Freund's complete adjuvant containing 100 μg of PLP(139–151) and 200 μg of *M. tuberculosis* H37Ra followed 2 h later with 200 ng of pertussis toxin delivered intraperitoneally. *R(+)*WIN55,212-2 (20 mg/kg) was administered intraperitoneally on days 0, 1, 2, 3, 4, and 5. GW6471 (10 mg/kg) was administered intraperitoneally on days 0, 1, 2, 4, and 6 after PLP immunization. Control mice received Cremophor/PBS (20:80) as vehicle. Data are from 4–8 mice/group. The clinical scoring system was as follows: 0, normal; 1, limp tail or hind limb weakness; 2, limp tail and hind limb weakness; 3, partial hind limb paralysis; 4, complete hind limb paralysis; 5, moribund. *, $p < 0.05$; **, $p < 0.01$ compared with control animals. +, $p < 0.05$ compared with animals treated with *R(+)*WIN55,212-2 alone. *Error bars*, S.E.

regulates IFN-β expression by targeting the AP-1 transcription factor and the PRDIV enhancer element of the IFN-β promoter, and importantly, these effects are manifested in a PPARα-dependent manner. In addition, the protective effects of *R(+)*WIN55,212-2 during the acute phase of EAE were ameliorated by GW6471. Hence, these data identify PPARα as a key receptor target for *R(+)*WIN55,212-2 in mediating the positive effects of the latter on IFN-β expression and highlight PPARα as a lead target to exploit in diseases, such as MS, that would benefit from augmentation of IFN-β expression.

IFN-β therapy is a current first line treatment of MS, decreasing relapse rate and modestly reducing disability accumulation (1). The mechanism(s) of action of IFN-β is complex with demonstrated effects on antigen presentation, co-stimulatory molecule expression, T cell proliferation, and leukocyte migration (5). The cell type-specific production of type I IFNs is controlled by the innate immune pattern recognition receptors, namely TLRs and retinoic acid-inducible gene I-like receptors (42). TLRs induce signaling via recruitment of the adaptor myeloid differentiation factor 88 (MyD88), with the exception of TLR3, which induces Myd88-independent signaling via Toll interleukin-1 receptor-domain-containing adaptor-inducing IFN-β (TRIF) protein (43). Such TRIF-mediated signaling promotes the phosphorylation and nuclear localization of tran-

scription factors IRF3 and IRF7 and subsequent induction of type I IFNs (23, 44). We have recently demonstrated that *R(+)*WIN55,212-2 can impact this pathway, acting as a novel regulator of TLR3 and TLR4 signaling by inhibiting the proinflammatory signaling axis triggered by TLR3 and TLR4 while selectively augmenting TLR3-induced activation of IRF3 and expression of IFN-β (8). This is consistent with data indicating that the plant-derived cannabinoids (45–46), endocannabinoids (30), and synthetic cannabinoid receptor agonists (30, 47–48) abrogate TLR4-induced proinflammatory mediator production in glia.

Much data indicate that cannabinoids, both synthetic and plant-derived, manifest at least some effects via PPARs. Such effects include palmitoylethanolamide-induced blunting of β-amyloid-induced inflammation (49), *R(+)*methanandamide-(50) and tetrahydrocannabinol-induced apoptosis (51), cannabidiol- and tetrahydrocannabinol-induced vasorelaxation (52, 53), *N*-oleoylethanolamine-induced protection following middle cerebral artery occlusion (13), and ajulemic acid-induced fibroblast differentiation and IL-8 promoter activity inhibition (14). In addition, data presented herein demonstrate such PPAR dependence for the synthetic cannabinoid *R(+)*-WIN55,212-2 both *in vitro* and *in vivo*. *R(+)*WIN55,212-2 belongs to the family of aminoalkylindoles that possess canna-

bimimetic properties despite being structurally dissimilar to plant-derived cannabinoids (54). However, although $R(+)$-WIN55,212-2 displays high affinity for both CB_1 and CB_2 cannabinoid receptors, with moderate selectivity for CB_2 (9), we (8, 37) and others (30–32, 55–57) have demonstrated cannabinoid receptor-independent effects of this aminoalkylindole. Indeed, our findings are consistent with PPAR-dependent effects of $R(+)$WIN55,212-2 on cell viability (58, 59) and adhesion molecule expression (60). It is noteworthy that Mestre *et al.* (60) demonstrated that $R(+)$WIN55,212-2 regulates endothelial expression of VCAM-1 adhesion molecule independent of CB_1 and CB_2 receptors, but involvement of PPAR receptors was identified, further demonstrating a non-cannabinoid-dependent effect for this aminoalkylindole. The selectivity of $R(+)$WIN55,212-2 in targeting PPARα independently of CB_1 or CB_2 is further supported by data indicating that ligands (pyrazol fatty acid amides) incorporating cannabinoid and PPARα features may lack cannabinoid activity (hypothermia and locomotor activity) but behave as potent activators of PPARs (61).

The concentrations of $R(+)$WIN55,212-2 used are in line with those used in various anti-inflammatory paradigms *in vitro* (30–32). Furthermore, the inability of the enantiomeric form of $R(+)$WIN55,212-2 to mimic its effects argues for a stereoselective receptor-mediated process(es), and the present study provides strong evidence for a role for PPARα. Indeed, recent studies have pointed to a growing importance for PPARs in regulating TLR signaling. Thus, PPARγ ligands negatively impact TLR-induced inflammatory signaling in glia (62), monocytes (63), and macrophages (64), and recently PPARγ has been shown to negatively regulate induction of IFN-β in response to TLR3 and TLR4 stimulation (65). Furthermore, in vascular smooth muscle cells, fenofibrate blunts TLR4-induced activation of TRIF and IRF3 (66). Because $R(+)$WIN55,212-2 (13, 38) and other cannabinoid-based compounds (38, 67) have been shown to bind and increase the transactivation capacity of PPARα, this receptor was selected as a potential lead target for mediating the effects of $R(+)$WIN55,212-2 on IFN-β expression. Using the PPARα antagonist GW6471, we confirm that $R(+)$WIN55,212-2 regulates PPARα transactivation to impart its regulatory role on IFN-β expression.

Fenofibrate exerts neuroprotective properties in rodent models of stroke (68), MS (69), and traumatic brain injury (70). Mechanistically, the activation of PPARα has been shown to inhibit proinflammatory gene transcription by repressing the pivotal inflammatory transcription factor, NF-κB (71), and this is supported by our findings indicating an inhibitory effect of fenofibrate on poly(I:C) induction of the NF-κB reporter gene. It is noteworthy that the PPARγ or PPARδ agonists, ciglitazone and L-165,041, did not negatively regulate poly(I:C) induction of the NF-κB reporter gene (supplemental Fig. 3), identifying activators of the α subtype as potent inhibitors of this transcription factor. The present study also adds further complexity to the mechanism of action of PPARα ligands, and the findings raise the possibility that the positive effects of PPARα on TLR3-induced expression of IFN-β may contribute to its *in vivo* effects. Indeed, data presented herein indicate that mice treated with $R(+)$WIN55,212-2 showed reduced severity of EAE dur-

ing both the first and second paralytic episodes. However, mice co-treated with $R(+)$WIN55,212-2 and GW6471 showed reduced protection during the first paralytic episode, indicating that the effects of $R(+)$WIN55,212-2 display some PPARα dependence during this phase of the disease. An imbalance in the cytokine network has a role in the initiation of EAE, with $CD4^+$ T helper 1 (Th1) cells and Th_{17} T cells suggested as having distinct and possibly complementary roles in disease onset (72). Both cannabinoid (73) and PPARα receptors (74) are expressed on T cells, and given that $R(+)$WIN55,212-2 may exert its anti-inflammatory properties in EAE by regulating T cell viability (56), whereas fenofibrate can regulate IL-17 and interferon-γ expression in isolated T cells (75), it will be interesting to mechanistically delineate the role of PPARs in mediating the effects of cannabinoids in EAE.

The study highlights dual effects of $R(+)$WIN55,212-2 on PPARα in that it directly activates and also induces the expression of PPARα. Few data linking an alteration in the expression profile of PPARs with neuroinflammation are available. However, it is attractive to suggest that the anti-inflammatory effects of $R(+)$WIN55,212-2 may not be restricted to directly activating PPARα but may also be associated with its ability to regulate the expression profile of PPARs and so facilitate increased signaling by endogenous PPAR ligands. Indeed, the ability of $R(+)$WIN55,212-2 to up-regulate the expression of PPARα adds to previous studies describing a similar effect of this aminoalkylindole on PPARγ expression (58, 59), suggesting that the impact of $R(+)$WIN55,212-2 on proliferative and inflammatory pathways may be due to its effects on PPAR expression. It is also noteworthy that LPS can enhance PPARα expression (76), and evidence from our group suggests that endogenous PPARα expression is up-regulated in EAE spinal cord and in peripheral blood mononuclear cells isolated from MS patients (data not shown). Further experiments will determine if this represents an endogenous neuroprotective response, an attractive possibility given that an up-regulation in PPAR expression has been shown to inhibit proinflammatory signaling (77).

$R(+)$WIN55,212-2 has been linked to the activation of the mitogen-activated protein kinase (MAPK) family members, including ERK (78–80), p38 (58, 78, 81), and JNK (58, 81–82). In particular, the ability of $R(+)$WIN55,212-2 to activate JNK in the CNS (82) is consistent with our findings in astrocytes. Using a specific JNK inhibitor, we demonstrate that this kinase is an upstream signaling intermediate targeted by $R(+)$WIN55,212-2 in the cascade leading to IFN-β expression. Furthermore, given that MAPK cascades phosphorylate different residues on the PPAR isoforms to control receptor activity (83), it will be of interest to determine the complex role of MAPKs in determining the effect of $R(+)$WIN55,212-2 on PPAR activation.

Our findings identify JNK phosphorylation and AP-1 activation as key mediators of the effects of $R(+)$WIN55,212-2 and the PPARα agonist fenofibrate. This is not without precedent because synthetic cannabinoids target AP-1 in the regulation of tyrosine hydroxylase gene transcription in neural cells (84), whereas administration of the endocannabinoid anandamide enhances AP-1 activity *in vivo* (85). Interestingly, the positive effects of $R(+)$WIN55,212-2 on AP-1 are mediated by PPARα,
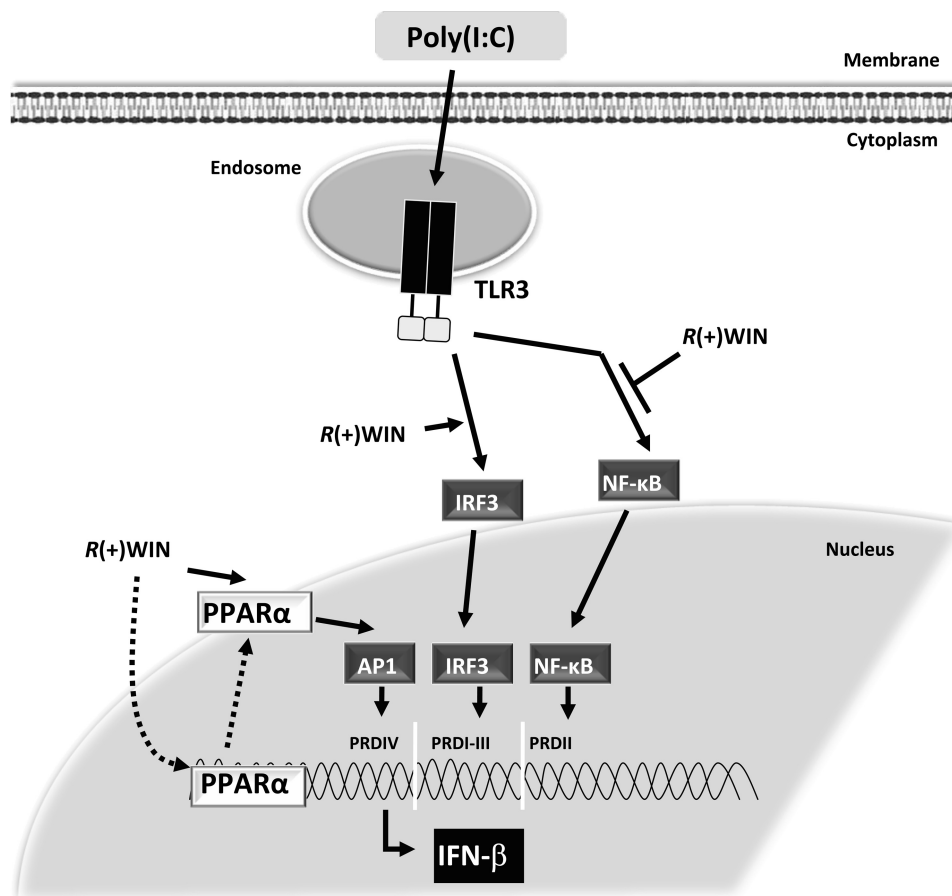
FIGURE 7. **Schematic representation of the mechanism by which *R*(+)WIN55,212-2 interacts with TLR3 signaling to regulate IFN-β expression in a PPARα-dependent manner.** We have previously demonstrated a dual mechanism of action of *R*(+)WIN55,212-2 (8). First, it can exert anti-inflammatory properties by down-regulating TLR-induced activation of NF-κB. In parallel, by enhancing activation of IRF3 and induction of IFN-β, it can boost an endogenous protective system. This study demonstrates that *R*(+)WIN55,212-2 targets the PRDIV domain of the IFN-β promoter by activating AP-1 in a PPARα-dependent manner. The study also highlights dual effects of *R*(+)WIN55,212-2 on PPARα in that it directly activates and also induces the expression of PPARα. *Pointed arrows*, activation; *blunt arrows*, inhibition.

and this is somewhat surprising given that evidence indicates that fenofibrate negatively regulates AP-1 activity in T cells (86) and vascular smooth muscle cells (87). Cell type specificity may account for this discrepancy, and further experiments will determine the mechanism by which *R*(+)WIN55,212-2-induced PPARα activation directly regulates JNK and AP-1 activation. It should be emphasized that not all of the effects of *R*(+)WIN55,212-2 on the IFN-β promoter are mediated by PPARα. Indeed, the former can augment TLR3-induced activation of IRF3 in a PPAR-independent manner, whereas, in contrast, fenofibrate inhibits activation of IRF3 in response to poly(I:C). Thus, whereas *R*(+)WIN55,212-2 employs PPARα to promote activation of AP-1 and the PRDIV domain of the IFN-β promoter, it can also utilize a PPARα-independent mechanism that overrides any negative regulatory effects of PPARα on IRF3 and the PRDI-III regions of the promoter.

In summary, our results show that *R*(+)WIN55,212-2 acts via PPARα to impact the JNK/AP-1 pathway, leading to activation of the PRDIV region of the IFN-β promoter (see Fig. 7). We also show that *R*(+)WIN55,212-2, in a PPARα-independent manner, can augment activation of IRF3 and the PRDI-III regions of the IFN-β promoter. Despite being mechanistically distinct, such effects of *R*(+)WIN55,212-2 on the PRDI-III and

PRDIV regions of the IFN-β promoter will result in positive cooperativity and strong induction of IFN-β. This adds significantly to our understanding of the mechanism(s) underlying the therapeutic effects of *R*(+)WIN55,212-2 in autoimmune disorders, in particular MS. More importantly, it also enhances PPARα as a lead therapeutic target to exploit in the treatment of diseases, like MS, that benefit from IFN-β augmentation.

REFERENCES
1. Graber, J. J., McGraw, C. A., Kimbrough, D., and Dhib-Jalbut, S. (2010) Overlapping and distinct mechanisms of action of multiple sclerosis therapies. *Clin. Neurol. Neurosurg.* **112,** 583–591
2. Goodin, D. S., and Bates, D. (2009) Treatment of early multiple sclerosis. The value of treatment initiation after a first clinical episode. *Mult. Scler.* **15,** 1175–1182
3. Jacobs, L. D., Cookfair, D. L., Rudick, R. A., Herndon, R. M., Richert, J. R., Salazar, A. M., Fischer, J. S., Goodkin, D. E., Granger, C. V., Simon, J. H., Alam, J. J., Bartoszak, D. M., Bourdette, D. N., Braiman, J., Brownscheidle, C. M., Coats, M. E., Cohan, S. L., Dougherty, D. S., Kinkel, R. P., Mass, M. K., Munschauer, F. E., 3rd, Priore, R. L., Pullicino, P. M., Scherokman, B. J., and Whitham, R. H. (1996) Intramuscular interferon β-1a for disease

progression in relapsing multiple sclerosis. The Multiple Sclerosis Collaborative Research Group (MSCRG) *Ann. Neurol.* **39,** 285–294

4. Li, D. K., and Paty, D. W. (1999) Magnetic resonance imaging results of the PRISMS trial. A randomized, double-blind, placebo-controlled study of interferon-β1a in relapsing-remitting multiple sclerosis. Prevention of relapses and disability by interferon-β1a subcutaneously in multiple sclerosis. *Ann. Neurol.* **46,** 197–206

5. Vosoughi, R., and Freedman, M. S. (2010) Therapy of MS. *Clin. Neurol. Neurosurg.* **112,** 365–385

6. Maniatis, T., Falvo, J. V., Kim, T. H., Kim, T. K., Lin, C. H., Parekh, B. S., and Wathelet, M. G. (1998) Structure and function of the interferon-β enhanceosome. *Cold Spring Harb. Symp. Quant. Biol.* **63,** 609–620

7. Noppert, S. J., Fitzgerald, K. A., and Hertzog, P. J. (2007) The role of type I interferons in TLR responses. *Immunol. Cell Biol.* **85,** 446–457

8. Downer, E. J., Clifford, E., Gran, B., Nel, H. J., Fallon, P. G., and Moynagh, P. N. (2011) Identification of the synthetic cannabinoid *R(+)*-WIN55,212-2 as a novel regulator of IFN regulatory factor 3 activation and IFN-β expression. Relevance to therapeutic effects in models of multiple sclerosis. *J. Biol. Chem.* **286,** 10316–10328

9. Howlett, A. C., Barth, F., Bonner, T. I., Cabral, G., Casellas, P., Devane, W. A., Felder, C. C., Herkenham, M., Mackie, K., Martin, B. R., Mechoulam, R., and Pertwee, R. G. (2002) International Union of Pharmacology. XXVII. Classification of cannabinoid receptors. *Pharmacol. Rev.* **54,** 161–202

10. Sharir, H., and Abood, M. E. (2010) Pharmacological characterization of GPR55, a putative cannabinoid receptor. *Pharmacol. Ther.* **126,** 301–313

11. Zygmunt, P. M., Petersson, J., Andersson, D. A., Chuang, H., Sørgård, M., Di Marzo, V., Julius, D., and Högestätt, E. D. (1999) Vanilloid receptors on sensory nerves mediate the vasodilator action of anandamide. *Nature* **400,** 452–457

12. O'Sullivan, S. E. (2007) Cannabinoids go nuclear. Evidence for activation of peroxisome proliferator-activated receptors. *Br. J. Pharmacol.* **152,** 576–582

13. Sun, Y., Alexander, S. P., Garle, M. J., Gibson, C. L., Hewitt, K., Murphy, S. P., Kendall, D. A., and Bennett, A. J. (2007) Cannabinoid activation of PPAR α. A novel neuroprotective mechanism. *Br. J. Pharmacol.* **152,** 734–743

14. Liu, J., Li, H., Burstein, S. H., Zurier, R. B., and Chen, J. D. (2003) Activation and binding of peroxisome proliferator-activated receptor γ by synthetic cannabinoid ajulemic acid. *Mol. Pharmacol.* **63,** 983–992

15. Straus, D. S., and Glass, C. K. (2007) Anti-inflammatory actions of PPAR ligands. New insights on cellular and molecular mechanisms. *Trends Immunol.* **28,** 551–558

16. Smeets, P. J., Teunissen, B. E., Planavila, A., de Vogel-van den Bosch, H., Willemsen, P. H., van der Vusse, G. J., and van Bilsen, M. (2008) Inflammatory pathways are activated during cardiomyocyte hypertrophy and attenuated by peroxisome proliferator-activated receptors PPARα and PPARδ. *J. Biol. Chem.* **283,** 29109–29118

17. Kota, B. P., Huang, T. H., and Roufogalis, B. D. (2005) An overview on biological mechanisms of PPARs. *Pharmacol. Res.* **51,** 85–94

18. Desvergne, B., and Wahli, W. (1999) Peroxisome proliferator-activated receptors. Nuclear control of metabolism. *Endocr. Rev.* **20,** 649–688

19. Heneka, M. T., and Landreth, G. E. (2007) PPARs in the brain. *Biochim. Biophys. Acta* **1771,** 1031–1045

20. Racke, M. K., and Drew, P. D. (2008) PPARs in neuroinflammation. *PPAR Res.* **2008,** 638356

21. Ramanan, S., Kooshki, M., Zhao, W., Hsu, F. C., and Robbins, M. E. (2008) PPARalpha ligands inhibit radiation-induced microglial inflammatory responses by negatively regulating NF-κB and AP-1 pathways. *Free Radic. Biol. Med.* **45,** 1695–1704

22. Ramirez, S. H., Heilman, D., Morsey, B., Potula, R., Haorah, J., and Persidsky, Y. (2008) Activation of peroxisome proliferator-activated receptor γ (PPARγ) suppresses Rho GTPases in human brain microvascular endothelial cells and inhibits adhesion and transendothelial migration of HIV-1-infected monocytes. *J. Immunol.* **180,** 1854–1865

23. Moynagh, P. N. (2005) TLR signaling and activation of IRFs. Revisiting old friends from the NF-κB pathway. *Trends Immunol.* **26,** 469–476

24. Lehnardt, S. (2010) Innate immunity and neuroinflammation in the CNS. The role of microglia in Toll-like receptor-mediated neuronal injury. *Glia* **58,** 253–263

25. Sorensen, P. S., Ross, C., Clemmesen, K. M., Bendtzen, K., Frederiksen, J. L., Jensen, K., Kristensen, O., Petersen, T., Rasmussen, S., Ravnborg, M., Stenager, E., and Koch-Henriksen, N. (2003) Clinical importance of neutralizing antibodies against interferon β in patients with relapsing-remitting multiple sclerosis. *Lancet* **362,** 1184–1191

26. Sagar, D. R., Kendall, D. A., and Chapman, V. (2008) Inhibition of fatty acid amide hydrolase produces PPAR-α-mediated analgesia in a rat model of inflammatory pain. *Br. J. Pharmacol.* **155,** 1297–1306

27. Downer, E. J., Cowley, T. R., Lyons, A., Mills, K. H., Berezin, V., Bock, E., and Lynch, M. A. (2010) A novel anti-inflammatory role of NCAM-derived mimetic peptide, FGL. *Neurobiol. Aging* **31,** 118–128

28. Xu, H. E., Stanley, T. B., Montana, V. G., Lambert, M. H., Shearer, B. G., Cobb, J. E., McKee, D. D., Galardi, C. M., Plunket, K. D., Nolte, R. T., Parks, D. J., Moore, J. T., Kliewer, S. A., Willson, T. M., and Stimmel, J. B. (2002) Structural basis for antagonist-mediated recruitment of nuclear co-repressors by PPARα. *Nature* **415,** 813–817

29. Bennett, B. L., Sasaki, D. T., Murray, B. W., O'Leary, E. C., Sakata, S. T., Xu, W., Leisten, J. C., Motiwala, A., Pierce, S., Satoh, Y., Bhagwat, S. S., Manning, A. M., and Anderson, D. W. (2001) SP600125, an anthrapyrazolone inhibitor of Jun N-terminal kinase. *Proc. Natl. Acad. Sci. U.S.A.* **98,** 13681–13686

30. Facchinetti, F., Del Giudice, E., Furegato, S., Passarotto, M., and Leon, A. (2003) Cannabinoids ablate release of TNFα in rat microglial cells stimulated with lypopolysaccharide. *Glia* **41,** 161–168

31. Germain, N., Boichot, E., Advenier, C., Berdyshev, E. V., and Lagente, V. (2002) Effect of the cannabinoid receptor ligand, WIN 55,212-2, on superoxide anion and TNF-α production by human mononuclear cells. *Int. Immunopharmacol.* **2,** 537–543

32. Nilsson, O., Fowler, C. J., and Jacobsson, S. O. (2006) The cannabinoid agonist WIN 55,212-2 inhibits TNF-α-induced neutrophil transmigration across ECV304 cells. *Eur. J. Pharmacol.* **547,** 165–173

33. Willson, T. M., Brown, P. J., Sternbach, D. D., and Henke, B. R. (2000) The PPARs. From orphan receptors to drug discovery. *J. Med. Chem.* **43,** 527–550

34. Atzei, P., Gargan, S., Curran, N., and Moynagh, P. N. (2010) Cactin targets the MHC class III protein IκB-like (IκBL) and inhibits NF-κB and interferon-regulatory factor signaling pathways. *J. Biol. Chem.* **285,** 36804–36817

35. Smith, P., Fallon, R. E., Mangan, N. E., Walsh, C. M., Saraiva, M., Sayers, J. R., McKenzie, A. N., Alcami, A., and Fallon, P. G. (2005) *Schistosoma mansoni* secretes a chemokine binding protein with antiinflammatory activity. *J. Exp. Med.* **202,** 1319–1325

36. Croxford, J. L., and Miller, S. D. (2003) Immunoregulation of a viral model of multiple sclerosis using the synthetic cannabinoid R+WIN55,212. *J. Clin. Invest.* **111,** 1231–1240

37. Curran, N. M., Griffin, B. D., O'Toole, D., Brady, K. J., Fitzgerald, S. N., and Moynagh, P. N. (2005) The synthetic cannabinoid *R(+)*WIN 55,212-2 inhibits the interleukin-1 signaling pathway in human astrocytes in a cannabinoid receptor-independent manner. *J. Biol. Chem.* **280,** 35797–35806

38. Sun, Y., Alexander, S. P., Kendall, D. A., and Bennett, A. J. (2006) Cannabinoids and PPARα signaling. *Biochem. Soc. Trans.* **34,** 1095–1097

39. Herzberg, U., Eliav, E., Bennett, G. J., and Kopin, I. J. (1997) The analgesic effects of R(+)-WIN 55,212–2 mesylate, a high affinity cannabinoid agonist, in a rat model of neuropathic pain. *Neurosci. Lett.* **221,** 157–160

40. Miralles, F., Parra, M., Caelles, C., Nagamine, Y., Félez, J., and Muñoz-Cánoves, P. (1998) UV irradiation induces the murine urokinase-type plasminogen activator gene via the c-Jun N-terminal kinase signaling pathway. Requirement of an AP1 enhancer element. *Mol. Cell Biol.* **18,** 4537–4547

41. Hasseldam, H., and Johansen, F. F. (2011) Cannabinoid treatment renders neurons less vulnerable than oligodendrocytes in experimental autoimmune encephalomyelitis. *Int. J. Neurosci.* **121,** 510–520

42. Takeuchi, O., and Akira, S. (2009) Innate immunity to virus infection. *Immunol. Rev.* **227,** 75–86

43. Medzhitov, R., Preston-Hurlburt, P., Kopp, E., Stadlen, A., Chen, C., Ghosh, S., and Janeway, C. A., Jr. (1998) MyD88 is an adaptor protein in

the hToll/IL-1 receptor family signaling pathways. *Mol. Cell* **2**, 253–258

44. Fitzgerald, K. A., McWhirter, S. M., Faia, K. L., Rowe, D. C., Latz, E., Golenbock, D. T., Coyle, A. J., Liao, S. M., and Maniatis, T. (2003) IKKε and TBK1 are essential components of the IRF3 signaling pathway. *Nat. Immunol.* **4**, 491–496

45. Puffenbarger, R. A., Boothe, A. C., and Cabral, G. A. (2000) Cannabinoids inhibit LPS-inducible cytokine mRNA expression in rat microglial cells. *Glia* **29**, 58–69

46. Kozela, E., Pietr, M., Juknat, A., Rimmerman, N., Levy, R., and Vogel, Z. (2010) Cannabinoids Δ(9)-tetrahydrocannabinol and cannabidiol differentially inhibit the lipopolysaccharide-activated NF-κB and interferon-β/STAT proinflammatory pathways in BV-2 microglial cells. *J. Biol. Chem.* **285**, 1616–1626

47. Froger, N., Orellana, J. A., Cohen-Salmon, M., Ezan, P., Amigou, E., Sáez, J. C., and Giaume, C. (2009) Cannabinoids prevent the opposite regulation of astroglial connexin43 hemichannels and gap junction channels induced by pro-inflammatory treatments. *J. Neurochem.* **111**, 1383–1397

48. Molina-Holgado, F., Molina-Holgado, E., Guaza, C., and Rothwell, N. J. (2002) Role of CB1 and CB2 receptors in the inhibitory effects of cannabinoids on lipopolysaccharide-induced nitric oxide release in astrocyte cultures. *J. Neurosci. Res.* **67**, 829–836

49. Scuderi, C., Esposito, G., Blasio, A., Valenza, M., Arietti, P., Steardo, L., Jr., Carnuccio, R., De Filippis, D., Petrosino, S., Iuvone, T., Di Marzo, V., and Steardo, L. (2011) Palmitoylethanolamide counteracts reactive astrogliosis induced by β-amyloid peptide. *J. Cell Mol. Med.* **15**, 2664–2674

50. Eichele, K., Ramer, R., and Hinz, B. (2009) *R*(+)-methanandamide-induced apoptosis of human cervical carcinoma cells involves a cyclooxygenase-2-dependent pathway. *Pharm. Res.* **26**, 346–355

51. Carroll, C. B., Zeissler, M. L., Hanemann, C. O., and Zajicek, J. P. (2012) Δ(9)-THC exerts a direct neuroprotective effect in a human cell culture model of Parkinson's disease. *Neuropathol. Appl. Neurobiol.*, in press

52. O'Sullivan, S. E., Kendall, D. A., and Randall, M. D. (2006) Further characterization of the time-dependent vascular effects of Δ9-tetrahydrocannabinol. *J. Pharmacol. Exp. Ther.* **317**, 428–438

53. O'Sullivan, S. E., Sun, Y., Bennett, A. J., Randall, M. D., and Kendall, D. A. (2009) Time-dependent vascular actions of cannabidiol in the rat aorta. *Eur. J. Pharmacol.* **612**, 61–68

54. Pacheco, M., Childers, S. R., Arnold, R., Casiano, F., and Ward, S. J. (1991) Aminoalkylindoles. Actions on specific G-protein-linked receptors. *J. Pharmacol. Exp. Ther.* **257**, 170–183

55. Marchalant, Y., Rosi, S., and Wenk, G. L. (2007) Anti-inflammatory property of the cannabinoid agonist WIN-55212-2 in a rodent model of chronic brain inflammation. *Neuroscience* **144**, 1516–1522

56. Sánchez, A. J., González-Pérez, P., Galve-Roperh, I., and García-Merino, A. (2006) *R*-(+)-[2,3-Dihydro-5-methyl-3-(4-morpholinylmethyl)-pyrrolo-[1,2,3-de]-1,4-benzoxazin-6-yl]-1-naphtalenylmethanone (WIN-2) ameliorates experimental autoimmune encephalomyelitis and induces encephalitogenic T cell apoptosis. Partial involvement of the CB₂ receptor. *Biochem. Pharmacol.* **72**, 1697–1706

57. Smith, S. R., Terminelli, C., and Denhardt, G. (2000) Effects of cannabinoid receptor agonist and antagonist ligands on production of inflammatory cytokines and anti-inflammatory interleukin-10 in endotoxemic mice. *J. Pharmacol. Exp. Ther.* **293**, 136–150

58. Giuliano, M., Pellerito, O., Portanova, P., Calvaruso, G., Santulli, A., De Blasio, A., Vento, R., and Tesoriere, G. (2009) Apoptosis induced in HepG2 cells by the synthetic cannabinoid WIN. Involvement of the transcription factor PPARγ. *Biochimie* **91**, 457–465

59. Pellerito, O., Calvaruso, G., Portanova, P., De Blasio, A., Santulli, A., Vento, R., Tesoriere, G., and Giuliano, M. (2010) The synthetic cannabinoid WIN 55,212-2 sensitizes hepatocellular carcinoma cells to tumor necrosis factor-related apoptosis-inducing ligand (TRAIL)-induced apoptosis by activating p8/CCAAT/enhancer-binding protein homologous protein (CHOP)/death receptor 5 (DR5) axis. *Mol. Pharmacol.* **77**, 854–863

60. Mestre, L., Docagne, F., Correa, F., Loría, F., Hernangómez, M., Borrell, J., and Guaza, C. (2009) A cannabinoid agonist interferes with the progression of a chronic model of multiple sclerosis by down-regulating adhesion molecules. *Mol. Cell Neurosci.* **40**, 258–266

61. Alvarado, M., Goya, P., Macías-González, M., Pavón, F. J., Serrano, A.,

Jagerovic, N., Elguero, J., Gutiérrez-Rodríguez, A., García-Granda, S., Suardíaz, M., and Rodríguez de Fonseca, F. (2008) Antiobesity designed multiple ligands. Synthesis of pyrazole fatty acid amides and evaluation as hypophagic agents. *Bioorg. Med. Chem.* **16**, 10098–10105

62. Gurley, C., Nichols, J., Liu, S., Phulwani, N. K., Esen, N., and Kielian, T. (2008) Microglia and astrocyte activation by Toll-like receptor ligands. Modulation by PPAR-γ agonists. *PPAR Res.* **2008**, 453120

63. Dasu, M. R., Park, S., Devaraj, S., and Jialal, I. (2009) Pioglitazone inhibits Toll-like receptor expression and activity in human monocytes and db/db mice. *Endocrinology* **150**, 3457–3464

64. Ogawa, S., Lozach, J., Benner, C., Pascual, G., Tangirala, R. K., Westin, S., Hoffmann, A., Subramaniam, S., David, M., Rosenfeld, M. G., and Glass, C. K. (2005) Molecular determinants of cross-talk between nuclear receptors and Toll-like receptors. *Cell* **122**, 707–721

65. Zhao, W., Wang, L., Zhang, L., Yuan, C., Kuo, P. C., and Gao, C. (2010) Differential expression of intracellular and secreted osteopontin isoforms by murine macrophages in response to Toll-like receptor agonists. *J. Biol. Chem.* **285**, 20452–20461

66. Ji, Y., Wang, Z., Li, Z., and Liu, J. (2010) Modulation of LPS-mediated inflammation by fenofibrate via the TRIF-dependent TLR4 signaling pathway in vascular smooth muscle cells. *Cell Physiol. Biochem.* **25**, 631–640

67. Lo Verme, J., Fu, J., Astarita, G., La Rana, G., Russo, R., Calignano, A., and Piomelli, D. (2005) The nuclear receptor peroxisome proliferator-activated receptor-α mediates the anti-inflammatory actions of palmitoylethanolamide. *Mol. Pharmacol.* **67**, 15–19

68. Deplanque, D., Gelé, P., Pétrault, O., Six, I., Furman, C., Bouly, M., Nion, S., Dupuis, B., Leys, D., Fruchart, J. C., Cecchelli, R., Staels, B., Duriez, P., and Bordet, R. (2003) Peroxisome proliferator-activated receptor-α activation as a mechanism of preventive neuroprotection induced by chronic fenofibrate treatment. *J. Neurosci.* **23**, 6264–6271

69. Xu, J., Storer, P. D., Chavis, J. A., Racke, M. K., and Drew, P. D. (2005) Agonists for the peroxisome proliferator-activated receptor-α and the retinoid X receptor inhibit inflammatory responses of microglia. *J. Neurosci. Res.* **81**, 403–411

70. Besson, V. C., Chen, X. R., Plotkine, M., and Marchand-Verrecchia, C. (2005) Fenofibrate, a peroxisome proliferator-activated receptor α agonist, exerts neuroprotective effects in traumatic brain injury. *Neurosci. Lett.* **388**, 7–12

71. Poynter, M. E., and Daynes, R. A. (1998) Peroxisome proliferator-activated receptor α activation modulates cellular redox status, represses nuclear factor-κB signaling, and reduces inflammatory cytokine production in aging. *J. Biol. Chem.* **273**, 32833–32841

72. Park, H., Li, Z., Yang, X. O., Chang, S. H., Nurieva, R., Wang, Y. H., Wang, Y., Hood, L., Zhu, Z., Tian, Q., and Dong, C. (2005) A distinct lineage of CD4 T cells regulates tissue inflammation by producing interleukin 17. *Nat. Immunol.* **6**, 1133–1141

73. Börner, C., Höllt, V., and Kraus, J. (2007) Activation of human T cells induces up-regulation of cannabinoid receptor type 1 transcription. *Neuroimmunomodulation* **14**, 281–286

74. Dunn, S. E., Ousman, S. S., Sobel, R. A., Zuniga, L., Baranzini, S. E., Youssef, S., Crowell, A., Loh, J., Oksenberg, J., and Steinman, L. (2007) Peroxisome proliferator-activated receptor (PPAR)α expression in T cells mediates gender differences in development of T cell-mediated autoimmunity. *J. Exp. Med.* **204**, 321–330

75. Lee, J. W., Bajwa, P. J., Carson, M. J., Jeske, D. R., Cong, Y., Elson, C. O., Lytle, C., and Straus, D. S. (2007) Fenofibrate represses interleukin-17 and interferon-γ expression and improves colitis in interleukin-10-deficient mice. *Gastroenterology* **133**, 108–123

76. Mohapatra, S. K., Cole, L. E., Evans, C., Sobral, B. W., Bassaganya-Riera, J., Hontecillas, R., Vogel, S. N., and Crasta, O. R. (2010) Modulation of hepatic PPAR expression during Ft LVS LPS-induced protection from *Francisella tularensis* LVS infection. *BMC Infect. Dis.* **10**, 10

77. Li, P., Zhu, Z., Lu, Y., and Granneman, J. G. (2005) Metabolic and cellular plasticity in white adipose tissue. II. Role of peroxisome proliferator-activated receptor-α. *Am. J. Physiol. Endocrinol. Metab.* **289**, E617–E626

78. Yang, H., Wang, Z., Capó-Aponte, J. E., Zhang, F., Pan, Z., and Reinach, P. S. (2010) Epidermal growth factor receptor transactivation by the can-

nabinoid receptor (CB1) and transient receptor potential vanilloid 1 (TRPV1) induces differential responses in corneal epithelial cells. *Exp. Eye Res.* **91,** 462–471

79. Park, J. M., Xian, X. S., Choi, M. G., Park, H., Cho, Y. K., Lee, I. S., Kim, S. W., and Chung, I. S. (2011) Antiproliferative mechanism of a cannabinoid agonist by cell cycle arrest in human gastric cancer cells. *J. Cell Biochem.* **112,** 1192–1205

80. Moranta, D., Esteban, S., and García-Sevilla, J. A. (2007) Acute, chronic, and withdrawal effects of the cannabinoid receptor agonist WIN55212-2 on the sequential activation of MAPK/Raf-MEK-ERK signaling in the rat cerebral frontal cortex. Short term regulation by intrinsic and extrinsic pathways. *J. Neurosci. Res.* **85,** 656–667

81. Luca, T., Di Benedetto, G., Scuderi, M. R., Palumbo, M., Clementi, S., Bernardini, R., and Cantarella, G. (2009) The CB1/CB2 receptor agonist WIN-55,212-2 reduces viability of human Kaposi's sarcoma cells *in vitro*. *Eur. J. Pharmacol.* **616,** 16–21

82. Alvaro-Bartolomé, M., Esteban, S., García-Gutiérrez, M. S., Manzanares, J., Valverde, O., and García-Sevilla, J. A. (2010) Regulation of Fas receptor/Fas-associated protein with death domain apoptotic complex and associated signaling systems by cannabinoid receptors in the mouse brain. *Br. J.*

Pharmacol. **160,** 643–656

83. Gelman, L., Michalik, L., Desvergne, B., and Wahli, W. (2005) Kinase signaling cascades that modulate peroxisome proliferator-activated receptors. *Curr. Opin. Cell Biol.* **17,** 216–222

84. Bosier, B., Hermans, E., and Lambert, D. M. (2009) Concomitant activation of adenylyl cyclase suppresses the opposite influences of CB$_1$ cannabinoid receptor agonists on tyrosine hydroxylase expression. *Biochem. Pharmacol.* **77,** 216–227

85. DeMorrow, S., Francis, H., Gaudio, E., Ueno, Y., Venter, J., Onori, P., Franchitto, A., Vaculin, B., Vaculin, S., and Alpini, G. (2008) Anandamide inhibits cholangiocyte hyperplastic proliferation via activation of thioredoxin 1/redox factor 1 and AP-1 activation. *Am. J. Physiol. Gastrointest. Liver Physiol.* **294,** G506–G519

86. Cheng, S. M., Chu, K. M., and Lai, J. H. (2010) The modulatory mechanisms of fenofibrate on human primary T cells. *Eur. J. Pharm. Sci.* **40,** 316–324

87. Ryoo, S., Won, M., Kim, D. U., Kim, L., Han, G., Park, S. K., Mukaida, N., Maeng, P., Yoo, H. S., and Hoe, K. L. (2004) PPARα activation abolishes LDL-stimulated IL-8 production via AP-1 deactivation in human aortic smooth muscle cells. *Biochem. Biophys. Res. Commun.* **318,** 329–334